Optics & Laser Technology 47 (2013) 372–378

Contents lists available at SciVerse ScienceDirect

Optics & Laser Technology

journal homepage: www.elsevier.com/locate/optlastec

Effects of phase errors on phase locking of all-fiber laser arrays

Jie Li, Jianqiu Cao*, Xiaojun Xu

College of Optoelectronic Science and Engineering, National University of Defense Technology, Changsha, Hunan 410073, PR China

ARTICLE INFO

Article history:
Received 30 August 2011
Received in revised form
12 July 2012
Accepted 13 July 2012
Available online 30 October 2012

Keywords:
Fiber laser arrays
Phase locking
Phase errors

ABSTRACT

The effects of phase errors on phase locking of the all-fiber laser array are discussed. By analyzing the 5-fiber laser array, it is found that the phase properties of the array depend on the order of the magnitude of the inevitable random phase errors in the fiber lasers. The dynamics of maximum phase deviations are also traced to seek the condition of phase locking for the 5-fiber laser arrays. The results indicate that the random phase errors in the fiber lasers are required to be as small as 10^{-7} to ensure coherent beam combining of the array with a high efficiency. The 10- and 19-fiber laser arrays are also investigated, and the results are identical to those of the 5-fiber laser array. With the increase in the number of fiber lasers, "quasi-in-phase" state can always be realized until the random phase errors are controlled in the range $(0,10^{-7})$.

1. Introduction

Fiber lasers have become more and more attractive due to its advantages of good beam quality, high efficiency and high reliability. IPG has developed a single mode fiber with 9.6kW output power [1]. However, the power upscaling of the single fiber laser is limited by the thermal damage and the nonlinear effects. Coherent beam combining technology is an effective choice to achieve high output power while simultaneously maintaining beam quality [2].

To realize the coherent beam combining of fiber lasers, it is required that these fiber lasers should be phase locked. This requirement can be achieved by two ways: active phase locking [3–8] and passive phase locking [9–19]. The array of passive phase locking is attractive because of its advantages prior to the one of active phase locking, such as the compactness, reliability, flexibility, etc. additionally, the passive array can be fabricated with the all-fiber configuration [9–16]. The tapered fused bundle array is just one sort of the passive all-fiber laser array [15,16]. The array is different from the other sort of the passive arrays in mainly three points. The first one is that there is no obvious element for supermode selection (which is different from the array discussed in [17–19]). The second one is that all the fiber lasers are only affected mutually in the tapered fused bundle section outside which they are operated individually, which is different from the multicore fiber lasers [13,14]. The third one is that the output port of the array owns the multicore configuration which is different from the array with the fiber couplers [16,20]. The unique configuration of the array may results in the unique dynamics behaviors. Thus, a number of studies were carried out on phase locking of the tapered fused bundle array.

A tapered fused bundle fiber array with seven fiber lasers has also been carried on in laboratory, and five fiber lasers were found to create an in-phase state when the lasers were turned on simultaneously [16]. To make a deep understanding of the all-fiber laser array, Rogers developed the dynamical model for high-gain fiber laser arrays, which discussed the effects of the gain and the coupling between the fiber lasers on the output coherence [21,22]. The model was also used in Ref. [23] to analyze the scalability and stability of the all-fiber laser array.

In spite of that, It should be noted that the impact of random phase errors (caused by the perturbation to the fiber length) on the output of the array was not considered in these references. This case seems too ideal to be practical. Besides that, based on the studies on some other sorts of the passive array, it was revealed that the random phase error might have an serious effect on phase locking of the array [24,25]. Can the fiber lasers of the tapered fused bundle array be phase-locked with the random phase errors? How do the random phase errors affect the output of the array? These questions are of great importance for further understanding the tapered fused bundle array. It is a pity that these questions are still not very clear at present. Detail studies are needed to answer these questions.

Therefore, in this paper, the effects of the random phase errors on the phase locking of the array are studied. The contents of this paper are as follows. In Section 2, the coupling model and the iterative maps are introduced. In Section 3, the relationship between the random phase errors and the phase locking of the 5-fiber laser array is revealed in detail. The same work is also carried on the 10- and 19-fiber laser arrays. The scalability of the

* Corresponding author.
E-mail address: jq_cao@126.com (J. Cao).

0030-3992/$ - see front matter © 2012 Elsevier Ltd. All rights reserved.
http://dx.doi.org/10.1016/j.optlastec.2012.07.016

array is also analyzed. Finally, Section 4 is a summary of the main results.

2. Theoretical analysis

2.1. System model

A model of *N*-fiber laser array coupler form is sketched in Fig. 1. The model contains fiber gratings, a number of fiber lasers, and an optical coupler. The reflection of the fiber gratings are nearly 100%. Various gain media may be used in the fiber lasers. The fiber lasers are independent of each other except the region labeled optical coupler ($c_- \le z \le L$), where the optical fields of fiber lasers interact with each other. The single output face acting as the output reflector has a small reflectivity r in practice.

The dynamic equations of each fiber laser could be written in the form of iterative maps [21,22]

$$E_n(t+T) = \sum_{m=1}^{N} A_{nm}(t)E_m(t) \tag{1}$$

$$G_n(t+T) = G_n(t) + \varepsilon\left[G_n^p(t) - G_n(t)\right] - \frac{2\varepsilon}{I_{sat}}\left(1-e^{-G_n(t)}\right)I_n(t) \tag{2}$$

where $E_n(t)$ and $G_n(t)$ represent the electric field and the gain of the nth fiber laser of the array, ε is the ratio of the cavity round-trip time T to the fiber laser fluorescence time τ_s, I_{sat} is the saturation intensity ($I_{sat}=h\nu/\sigma_s\tau_s$ where ν is the laser oscillating frequency and σ_s is the stimulated emission cross section), $G_n^p$is the pump parameter for the nth fiber laser. The iterated map description will be valid as long as the gain G_n changes slowly with respect to the round-trip time. A_{nm} is the revolution operator of the round-trip field,

$$A_{nm} = r\sum_l S_{nl}e^{G_n + j\phi_n}S_{lm} \tag{3}$$

Here S is the coupling matrix describing the field evolution in the coupling region ($c_- \le z \le L$), ϕ_n is the round-trip phase shift in the region ($0 \le z \le c_-$), e^{Gn} is the field amplification of the nth fiber laser, and r is the field reflection coefficient at the output face. The essential part to perform the analysis of the all-fiber array is to determine the coupling matrix S_{ij}.

2.2. The region of coupling

According to the coupled mode theory [26] and the cross talk theory [27], the fields in the coupling region can be expressed as follows:

$$\frac{dE_n}{dz} - j(\beta_n + C_{nn})E_n = j\sum_{m=1,m\ne n}^{N} C_{nm}E_m \tag{4}$$

where β_n is the propagation constant of the nth fiber, C_{nm} is the cross-coupling coefficient, and C_{nn} is the self-coupling coefficient, which can be negligible compared with C_{nm} and ignored in this paper. So, Eq. (4) is simplified as

$$\frac{dE_n}{dz} = jME \tag{5}$$

where $M_{kk}=\beta_n$, and $M_{kl}= C_{kl}$ for $k \ne l$. It is assumed that all fiber lasers are identical and the coupling between two adjacent fibers are same, therefore, $\beta_n = \beta$, $C_{kl} = \kappa$. The coupling generator matrix M can be written as$M_{nm} = \beta\delta_{nm} + \kappa(1-\delta_{nm})$, where δ is Kronecker symbol. Assuming that N is equal to 5, M can be written as

$$M = \begin{bmatrix} \beta & \kappa & \kappa & \kappa & \kappa \\ \kappa & \beta & \kappa & \kappa & \kappa \\ \kappa & \kappa & \beta & \kappa & \kappa \\ \kappa & \kappa & \kappa & \beta & \kappa \\ \kappa & \kappa & \kappa & \kappa & \beta \end{bmatrix} \tag{6}$$

M is symmetric and M does not depend on z over its entire length. So the coupling matrix S is expressed as

$$S = \exp(jML) \tag{7}$$

where L is the length of the coupler.

Since M is a circulant [28], it can be diagonalized by a unitary transformation $U = \exp(-j2\pi kl/N)$. Then, S can be expressed as [22]

$$\begin{aligned} S_{nm} &= [U(U^*SU)U^*]_{nm} = [U\exp(jLU^*MU)U^*]_{nm} \\ &= \frac{1}{N}e^{iL(\beta-k)}\left[\left(e^{iNL\kappa}-1\right) + N\delta_{n,m}\right] \end{aligned} \tag{8}$$

With the Eqs. (1) and (2) numerically solved, the temporal dynamics of the optical fields and the phase properties of the fiber laser can be obtained.

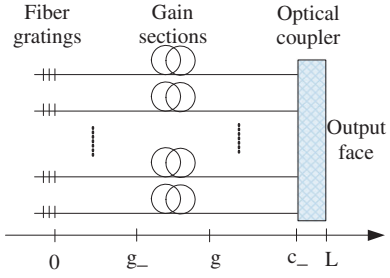

Fig. 1. Schematic of the fiber laser array.

3. Numerical calculation and discussion

In the former studies, the phase-locking state of the fiber laser arrays have been investigated preliminarily [21,23]. In order to verify our numerical simulation, we repeat the simulation carried out in Ref. [23] in the case of the five-laser array. The parameters used in the simulation are given in Table 1, and the results are given in Fig. 2. Fig. 2(a) depicted the dynamic behavior for the output power intensity of the laser array field, and it can be seen that the output intensity reaches a stable output after the initial fluctuation. Fig. 2(b) further traces 9865–9880 iterations of one stable state section and the relative phases between array elements are constant, which implies that fiber laser array are locked mutually and has the ability to achieve in-phase state

Table 1
Parameters of the simulation.

Wavelength (nm)	1060
Core numerical aperture	0.06
Cladding numerical aperture	0.46
Core diameter (μm)	20
Core reflectivity	1.4668
Cladding reflectivity	1.4656
ε	$\sim 10^{-4}$
radiation cross section (σ_s)	1×10^{-25}
florescence time (τ_s)	1 ms
saturation intensity (I_{sat})	1.87×10^{-9} W/m^2
Pumping parameter ($G_n^p = G^p$)	2.5
output face reflectivity (r)	0.1
coupling length (L)	2 cm